BMC Pulmonary Medicine

RESEARCH

Open Access

Exosomes from Tregs mitigate lung damage caused by smoking via inhibiting inflammation and altering T lymphocyte subsets in COPD rats

Xuefang Tao[1], Hai Tian[2], Guowen Wang[1], Yongzhen Sun[1] and Liangyan Zhao[1*]

Abstract

Background Chronic obstructive pulmonary disease (COPD) is a common disease with respiratory symptoms and limited airflow. Exosomes derived from Tregs (Treg-exo) could regulate immune function and prevent autoimmune disease. This study assessed Treg-exo effects on COPD.

Methods In vivo, rats were divided into three groups including control, COPD and exosomes groups. COPD models were established by passive smoking combined with lipopolysaccharide. Phosphate buffered saline or Treg-exo were administered via tail vein. Lung function, Hematoxylin and Eosin staining, and enzyme-linked immunosorbent assay (ELISA) were performed to evaluate lung function, histopathology and inflammation. Flow cytometry was used for peripheral blood T cell separation and counting. In vitro, COPD cluster of differentiation (CD) 4^+ T-cells were isolated from spleen and co-cultured with Treg-exo alone or in combination with Colivelin (a signal transducer and activator of transcription 3/STAT3 activator). Flow cytometry, ELISA, and Western blot were used to count T helper cell 17 (Th17) and detected cytokines and STAT3 proteins expression.

Results In vivo, pulmonary function tests and HE staining showed Treg-exo treatment enhanced lung function and alleviated lung damage; flow cytometry showed Treg-exo treatment decreased $CD8^+$, $CD4^+$ $CD25^-$ cells and Th17; ELISA assay found Treg-exo treatment increased transforming growth factor-β and interleukin (IL)-10 and decreased tumor necrosis factor-α and IL-8 in serum, broncho alveolar lavage fluid, and lung tissue. In vitro, Treg-exo treatment inhibited Th17 differentiation and suppressed the content of IL-6, IL-17, and IL-23 and STAT3 phosphorylation.

Conclusions Treg-exo suppressed inflammation and $CD4^+$ T-cell differentiation to Th17, possibly by inhibiting STAT3 phosphorylation.

*Correspondence:
Liangyan Zhao
0052019118@usx.edu.cn

Full list of author information is available at the end of the article

Graphical abstract

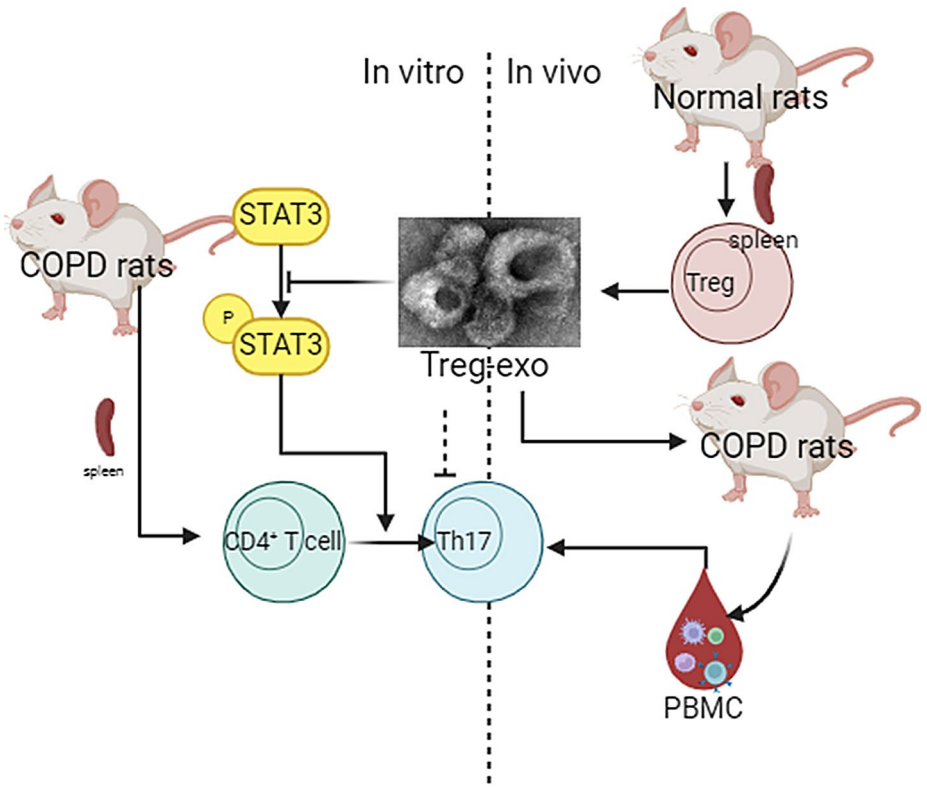

Keywords T lymphocyte subset, Exosomes, Chronic obstructive pulmonary disease, Lung tissue remodeling, Immune response

Background

Chronic obstructive pulmonary disease (COPD) is a chronic inflammatory disease, encompassing many clinical phenotypes [1]. In particular, airway remodeling, leading to a condition known as 'obstructive bronchitis and bronchiolitis', is central to COPD, characterized by small airway narrowing and physiological [2]. As in previous studies [3, 4], smoking was the main risk factor for COPD and inflammatory response was widely recognized as the primary underlying mechanism [5]. Briefly, when exposed to toxic particles in smoking, depleted endogenous antioxidant defenses occur, leading to damage to airway and lung epithelial cells [6, 7]. In addition, smoking also activated many biological processes, such as epithelial-mesenchymal transition (EMT) and immune response, constriction and remodeling of the airway [8, 9].

Moreover, cluster of differentiation (CD) 4^+ T-cells, a subset of T-lymphocytes, are able to differentiate into a variety of cell types, such as T helper cell (Th)1, Th2, Th17, and Treg, following distinct cytokine regulation. Among these subsets of T-lymphocytes, Th1, Th2, and Th17 are significantly associated with COPD [10, 11]. Certain immunological imbalances are commonly observed in patients with COPD, such as an imbalance between Th1/Th2 and Th17/Treg [12, 13]. For example, smoking, a common risk factor for COPD, can disrupt the Th17/Treg balance, leading to Th17 stimulation and the release of inflammatory cytokines. Subsequently, this immune response and secondary chronic inflammation may contribute to COPD progression and worsening [14, 15].

Exosomes, a unique type of extracellular vesicles, have emerged as an important area of inquiry in the treatment of COPD due to their unique and diverse biological functions. Exosomes produced by different types of cells may have different roles in COPD pathogenesis. As in previous study, exosomes from Treg (Treg-exo) played a regulatory role in effector T cells [16], thus regulating the immune response. Another study showed that exosomes were involved in COPD development through the epithelial-mesenchymal transition [17]. For instance, researchers have shown that HOTAIRM1, from exosomes derived from human bronchial epithelial cells, can

promote differentiation and proliferation of primary lung fibroblasts, leading to excessive collagen secretion and airway obstruction [18]. Additionally, exosomes derived from immature dendritic cells have been reported to inhibit signal transducer and activator of transcription 3 (STAT3) phosphorylation, which is responsible for the differentiation of interleukin (IL)17$^+$ CD4$^+$ Th17. These exosomes instead stimulate the transformation of forkhead box protein P3$^+$ CD4$^+$ Tregs [19]. Moreover, it was widely acknowledged that STAT3 phosphorylation benefited to Th17 differentiation [20]. Thus, we hypothesized that Treg-exo may suppress Th17 differentiation by inhibiting STAT3 phosphorylation.

This study aimed to explore the effect of Treg-exo on COPD. We mainly assessed the changes in pro-inflammatory cytokines and T lymphocytes subsets and investigated whether exosomes regulated T lymphocytes subsets via STAT3 phosphorylation.

Methods

Animals

Thirty-two male Sprague Dawley rats (SPF grade, 200 g, 6 weeks old) were procured from Shanghai Jihui Experimental Animal Breeding Co., Ltd. (SCXK(Hu)2022-0009). The rats were maintained in a specific pathogen-free facility under the following conditions: a 12-h light/dark cycle, an ambient temperature of 22 ± 2 ℃, and a relative humidity of 55–60% (SYXK (zhe) 2021-0033). The Animal Experimentation Ethics Committee of Zhejiang Eyong Pharmaceutical Research and Development Center approved the ethical conduct of the animal experiments (ZJEY-20220818-01).

Lymphocyte separation

Eleven rats were used to isolate rat spleen as in previous studies [13, 21]. In brief, the rat abdomen was disinfected with 70% alcohol and then cut to obtain spleen. The spleen was placed in 1× phosphate buffered saline (PBS) buffer on ice, followed by grinding and filtration with sterile steel wire. After mixing with 500 μL Roswell Park memorial institute (RPMI) 1640 medium and centrifuged at 800×g for 30 min, lymphocyte layer was absorbed, washed with 10 mL RPMI 1640 medium. Subsequently, the sample was centrifuged at 250 g for 10 min to obtain lymphocytes, followed by resuspension and counting.

Isolation and culture of Tregs

The isolated cells were sorted through a magnetic bead method [22]. In summary, after incubation with antibody FITC CD25 (102005, Biolegend, China; 1:200), the cell suspension was sorted by magnetic-activated cell sorting separator (130-042-302, Miltenyi Biotec) and rinsed with 3 mL running buffer (130-091-211, Miltenyi Biotec) to obtain Tregs. Subsequently, flow cytometry successfully identified Tregs, followed by the addition of cryopreservation solution with 10% dimethyl sulfoxide for cryopreservation. Microbeads used were as follows: CD4 MicroBeads, rat (130-090-319); Anti-FITC MicroBeads (130-048-701). Both the MicroBeads were purchased from Miltenyi Biotec, Germany.

Flow cytometry

Flow cytometry was performed after resuspending the cells. After washing it twice with PBS, cells were resuspended in PBS. Then, antibodies of CD4, CD8, CD25, or IL-17 were added, followed by 30-min incubation in the dark. Subsequently, cells were washed twice again, then, they were centrifuged and resuspended. After screening cells using a 200-mesh screen, flow cytometry was performed on NovoCyte Flow Cytometer System (Agilent, USA). Cells were gated on SSC-H and CD4$^+$ cells, CD8$^+$ CD4$^-$ cells, CD4$^+$ CD25$^-$, and CD4$^+$ IL17$^+$ cells. The antibodies used in flow cytometry were as follows: CD4 antibody (sc-19641, Santa Cruz Biotechnology, USA; 1:20), CD8 antibody APC (sc-1177, Santa Cruz Biotechnology; 1:20), antibody FITC-CD25 (102005, Biolegend, China; 1:200), IL-17 PE antibody (sc-374218 Santa Cruz Biotechnology; 1:200).

Exosome extraction and identification from Tregs

Exosomes were extracted by ultracentrifugation method as previous study [23]. Briefly, Treg samples were gradually centrifuged in 2000 g at 4 ℃ for 30 min and then in 10,000×g at 4 ℃ for 45 min. Supernatant was filtered 0.45 μm membrane and then centrifuged in 100,000×g for 70 min at 4 ℃. After resuspending in 500 μL precooled 1× PBS, the isolated exosomes were identified by transmission electron microscope (TEM), nanoparticle tracking analysis (NTA), and Western blot.

TEM

20 μL sample dropwise to copper mesh for 1 min, stain with 10 μL uranium dioxide acetate, and absorb liquid with filter paper. Dry for a little while and image sample at 100 kV electron microscopy.

NTA

Exosome samples are diluted with 1× PBS for NTA detection with nanoparticle tracking analyzer (Zeta-VIEW, PARTICLE METRIX).

Western blot

5× radio-immunoprecipitation assay lysate buffer (20115, Yeasen, China) was added to exosome, mixed on ice for 30 min, then measured protein concentration with bicinchoninic acid assay. Sodium dodecyl sulfate-polyacrylamide gel electrophoresis and polyvinylidene fluoride transfer performed. Subsequently, members were sealed

with 5% skim milk. Primary antibodies were added, incubated at 4℃ overnight and then secondary antibody were incubated with members at room temperature 1 h. Then visualized with ECL reagents using gel imaging system (ChemiScope 3000mini, CLINX).

The antibodies used in Western blot were as follows: TSG101 antibody (DF8427, Affinity, USA; 1:1000); CD9 antibody (AF5139, Affinity; 1:1000); CD63 antibody (AF5117 Affinity; 1:1000); Anti-rabbit IgG, HRP-linked antibody (7074, CST, USA; 1:6000); β-actin antibody (81115-1-RR, Proteintech, China; 1:10000).

COPD construction and drug intervention

The COPD model was constructed via cigarette smoke exposure combined with endotracheal dripping of lipopolysaccharide (LPS) (60747ES, Yeasen, China) as a previous study [24]. Briefly, 18 rats were randomly divided into two groups, the control group ($n = 6$) and the model group ($n = 12$). On the 1st and 15th day, rats received 0.2 mL LPS (1 mg/mL) instillation in model group, while 0.2 mL saline in control group. Afterward, the rats in the model received passive smoking with 15 cigarettes in a homemade box twice daily for 30 min, excluding days 1 and 15. The COPD model was constructed for 5 weeks, while the rats in the control group breathed normal air.

Then, model rats were further divided into model and exosome groups. The dosage of exosomes referred to previous studies [25, 26]. Briefly, exosome group received about 30 μg Treg-exo (dissolved in 0.5 mL PBS) via tail vein injection daily for 2 weeks, while control and model groups received 0.5 mL PBS.

Pulmonary function test

Rats were anaesthetized with 2% pentobarbital sodium (50 mg/kg) and then fixed to a plate with supine. After the neck skin was cut to separate the trachea, a small incision was made in the upper section of the tracheal ring, allowing the tracheal intubation to be inserted and then fixed with surgical wire ligation.

Peak expiratory flow (PEF), airway resistance (RI), functional residual capacity (FRC), and dynamic lung compliance (Cdyn) were detected by the animal lung function testing system (EMKA-PLT-WBP, EMKA, France), repeated 3 times for each indicator.

Observation of pathological pulmonary tissue morphologies

Lung tissue was fixed in 4% paraformaldehyde for 24 h, followed by dehydration, transparency, waxing, embedding, slicing, stained with hematine-eosine (G1003, Servicebio, China), and sealing. Changes in bronchial and lung tissue were observed with optical microscopy.

Peripheral blood lymphocyte subsets cell count

Rat blood samples were added to Eppendorf tubes containing anticoagulant within 2 h. After centrifugation at 800×g for 20 min, the lymphocytes in the middle were absorbed by the dropper, then washed with PBS and centrifuged at 600×g for 10 min, twice. Subsequently, the supernatant was discarded and 100 μL PBS was added to resuspend cells. 2.5 μL corresponding antibodies were added to the cell suspension and then incubated at 4 °C in the dark for 30 min. After incubation, the cells were washed twice with PBS and resuspended with 200 μL of PBS. Before boarding the machine, the cells passed through a 200-mesh screen. Flow cytometry (NovoCyte, Agilent, USA)Agilent, USA) was performed after resuspending the cells.

Enzyme-linked immunosorbent assay (ELISA)

After anesthesia and then euthanasia, Blood, lung, and bronchoalveolar lavage fluid (BALF) were collected. Blood samples were collected from the heart and centrifuged at 1000×g for 10 min to obtain serum. Rats were perfused with PBS using endotracheal intubation to obtain BALF. During this process, the expansion of the lung lobes was closely monitored. Once the perfusion is complete, the syringe was gently withdrawn to collect the lavage fluid. This perfusion process was repeated 2–3 times to enrich the samples. Then, lung tissue was removed from rats and homogenized to obtain tissue homogenization.

Serum, tissue homogenate, BALF, and cell samples were centrifuged at 1000×g for 15 min to obtain the supernatant. The cytokines were then measured with corresponding kits as manufacturer's guidelines. The kits used in ELISA were all purchased from Jiangsu Meimian Industrial Co., Ltd and the article number were listed as follows: Transforming growth factor (TGF)-β ELISA kit (MM-20594R1, Meimian, China); tumor necrosis factor (TNF)-α ELISA kit (MM-0180R1, Meimian); interleukin (IL)-10 ELISA kit (MM-0195R1, Meimian); IL-8 ELISA kit (MM-0175R1, Meimian).

$CD4^+$ cell isolation from spleen and culture

Lymphocytes were isolated from 3 other COPD rats and $CD4^+$ T-cells were sorted by magnetic beads as described above. After identification by flow cytometry (NovoCyte, Agilent, USA), $CD4^+$ T-cells were divided into three groups: control, exosome and exosome + Colivelin groups.

The cells were stimulated by CD3 antibody (sc-70626, SANTA CRUZ; 1:100) and CD28 (sc-70626, SANTA CRUZ; 1:40) antibodies for T cell expansion as previous study [27]. The exosome and exosome + Colivelin groups were added 2 μL/mL exosomes while the control group was added 2 μL/mL PBS [25]. Meanwhile, 0.5 μM

Colivelin was added to exosome + Colivelin groups [28]. All groups were then co-cultured for 48 h. The cytokines and relative proteins were measured by ELISA and Western blot, respectively, as mentioned above.

The kits used in ELISA were as follows: IL-6 ELISA kit (RX302856R, Ruixin); IL-17 ELISA kit (RX302873R, Ruixin); IL-23 ELISA kit (RX302865R, Ruixin). The antibodies used in Western blot were listed as follows: β-actin antibody (81115-1-RR, Proteintech; 1:10000); signal transducer and activator of transcription 3 (STAT3) antibody (AF6294, Affinity; 1:1000); phosphorylated (p)-STAT3 antibody (AF3293, Affinity; 1:1000); IL-17 antibody (DF6127, Affinity; 1:1000).

Statistical analysis

Data was displayed as mean ± standard deviation. Normal distribution data was analyzed through one-way analysis of variance, followed by Turkey test for pairwise comparisons. For uneven variance, Dunnett's T3 was applied. For non-normal data, Kruskal Wallis H test was instead. Significance was determined by $p < 0.05$.

Results

Identification of exosomes from Tregs

To obtain Treg-exo, isolated lymphocyte cells were sorted. As shown in Fig. 1A, the T-lymphocyte population was predominantly concentrated in quadrant 2. These cells were therefore identified as Tregs, as they were characterized by their high expression of CD4 and CD25.

Subsequently, we used TEM, NTA, and Western blot to visualize and confirm Treg-exo. An apparition of tea tray-like vesicles with a double concave bilayer membrane structure was observed through TEM (Fig. 1B). In addition, NTA showed that the size distribution has an average diameter of 109.14 nm, within 150 nm, consistent with exosome characteristics (Fig. 1C). In addition, Western blot results confirmed the expression of exosome-specific marker proteins including CD63, CD9, and TSG101, indicating that exosomes were successfully extracted from Tregs (Fig. 1D) and their raw data were shown in supplementary Figure S1.

Exosome promoted the pulmonary function and mitigated lung tissue damage

To accurately assess the degree of impairment of lung function, we examined four key parameters: Cdyn, PEF, FRC, and RI. Compared to the health control group, our data confirmed a marked reduction in Cdyn and PEF in the model group. Our findings also indicated significant increases in FRC and RI. Altogether, these results point to severe impairment of lung function (Fig. 2A-D). However, we observed significant intervention and reversal of these trends after exosomes administration, indicating a positive impact on lung function.

Furthermore, HE staining was used to visualize pathological damage to lung tissue. As shown in Fig. 2E, bronchioles in the model group contrast with intact epithelial structure observed in the control group. Notably, these bronchioles showed significant constriction and irregularity, accompanied by thickened airway walls, which contributed to a narrow. In addition, these bronchioles were encircled by severe inflammatory infiltration, leading to cilia that were adhered, lodged, and shed. Remarkably, the damage was substantially reduced after exosome treatment.

Exosomes promoted T lymphocyte differentiation

To further investigate the impact of exosomes on lymphocytes, we used flow cytometry to assess the T lymphocyte phenotype isolated from peripheral blood mononuclear cell of rats. Our results showed a significant increase in $CD4^+$ T-cells, $CD8^+$ T cells, and Th17 post-COPD exposure, but exosome therapy was able to mitigate this trend (Fig. 3A-F).

Exosomes suppressed the inflammation response

We used ELISA to measure levels of various cytokines in serum (Fig. 4A-D), BALF (Fig. 4E-H), and lung tissue (Fig. 4I-L). Results showed a similar overall trend, with significant differences between the two groups. Specifically, TGF-β and IL-10 both decreased, while the levels of TNF-α and IL-8 were increased in the model group, suggesting an enhanced inflammatory response ($p < 0.01$). In contrast, exosomes treatment effectively mitigated these inflammatory responses.

Exosomes suppressed Th17 differentiation by inhibiting STAT3 phosphorylation

To address molecular mechanism underlying exosomes and Th17 differentiation, we investigated the effects of exosomes on $CD4^+$ T cells from COPD rats and STAT3 signaling pathway. As shown in Fig. 5A, we obtained $CD4^+$ T cells with 98.9% purity. Then, the results of flow cytometry assay showed that normal Treg-exo significantly inhibited the Th17 differentiation of $CD4^+$ T-cell ($p < 0.01$) (Fig. 5B, C). However, after being exposed to Colivelin, a STAT3 activator, the proportion of Th17 differentiation increased ($p < 0.01$).

Subsequently, cytokines including IL-6, IL-17, and IL-23 were detected to explore possible mechanisms using ELISA. As shown in Fig. 5D-F, all three cytokines showed a similar trend. That is, they decreased significantly in the exosome group, while Colivelin treatment resulted in an increase in cytokine content ($p < 0.05$), suggesting that the exosome effect was partially eliminated.

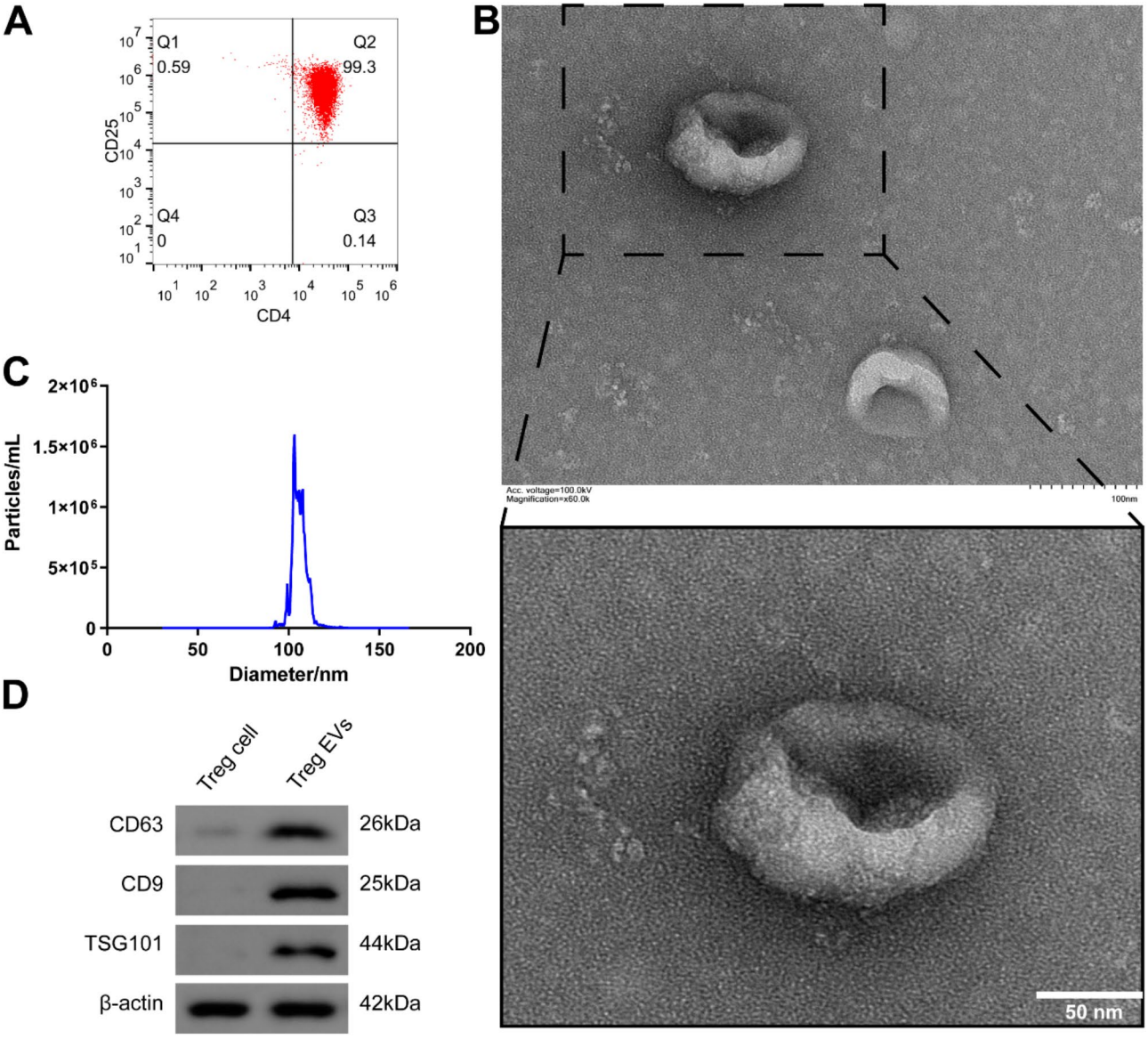

Fig. 1 Identification of exosomes from Tregs of Sprague Dawley rat spleen. (**A**) Flow cytometry was used to identify cells. Flow quadrant diagram of Tregs (quadrant 2). (**B**) Transmission electron microscope was used to observe morphology of exosomes and the representative images of exosomes under transmission electron microscope were **shown**. Magnification ×60k, scale bar = 100 and 50 nm. (**C**) Nanoparticle Tracking Analysis was used for particle size distribution of exosomes. There was a total of 21,714,571 events. $n = 5$. (**D**) Western blot was used to detect exosome biomarkers and there were representative band images of exosome biomarkers CD63, CD9, and TSG101. $n = 3$. The "*n*" means number of experimental replicates

Finally, relative protein expressions were detected to verify the connection between exosomes and STAT3 using Western blot (Fig. 5G-J). The total STAT3 levels showed no significant difference (Fig. 5G, J). We observed that exosomes inhibited p-STAT3 and reduced IL-17 expression ($p < 0.01$), while Colivelin significantly enhanced p-STAT3 and promoted IL-17 expression (Fig. 5H-J). Their raw data were shown in supplementary Figure S2. The decreased IL-17 expression in $CD4^+$ T cells treated with exosomes is correlated with STAT3 phosphorylation.

Discussion

In our study, we observed that exosomes derived from rat Tregs enable to enhance pulmonary function and alleviate lung tissue damage. In addition, exosomes also played a role in influencing T lymphocyte differentiation, which may relate to STAT3 pathway, thus mitigating inflammation in COPD model rats.

The hallmark of COPD is generally characterized by persistent respiratory symptoms and airflow limitations, an association that may be linked to a complex immune response and secondary chronic inflammation [29]. Di Stefano et al. reported that the important role

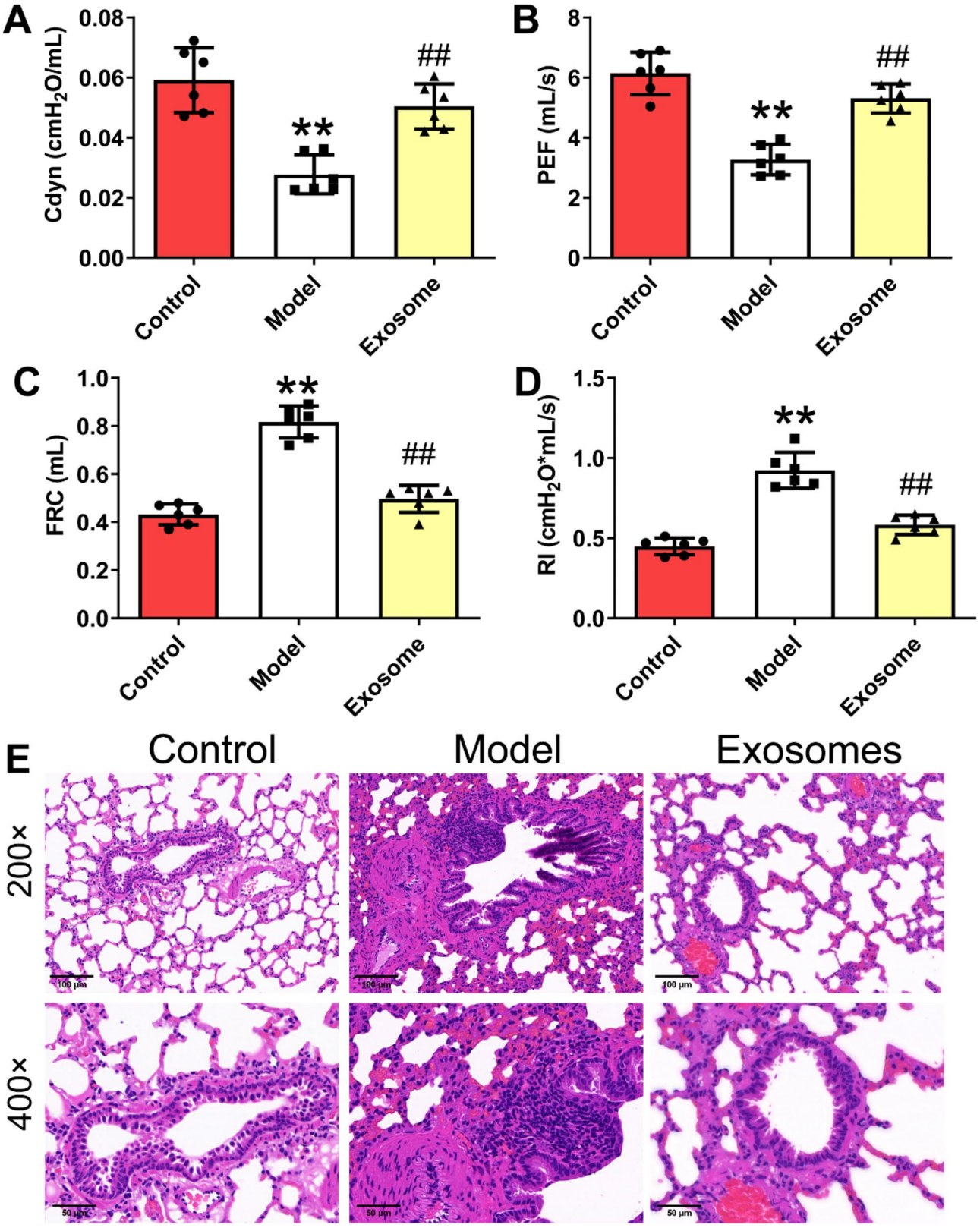

Fig. 2 Assessment of rat lung function and pulmonary histopathological changes. Lung function indicator of (**A**) Cdyn, (**B**) PEF, (**C**) FRC, and (**D**) RI. $n = 6$. Mean ± standard deviation, one-way analysis of variance was used for statistical analysis. (**E**) Representative images of Hematoxylin and Eosin staining from Sprague Dawley rat lung tissues. The images captured by the microscope for each group were collected at the same time under the same conditions. $n = 3$; Magnification ×200 and ×400, scale bar = 100 and 50 μm. PEF, peak expiratory flow; RI, airway resistance; FRC functional residual capacity; Cdyn, dynamic lung compliance. $^{**}p < 0.01$ vs. control group; $^{\#\#}p < 0.01$ vs. model group. The "*n*" means number of animals

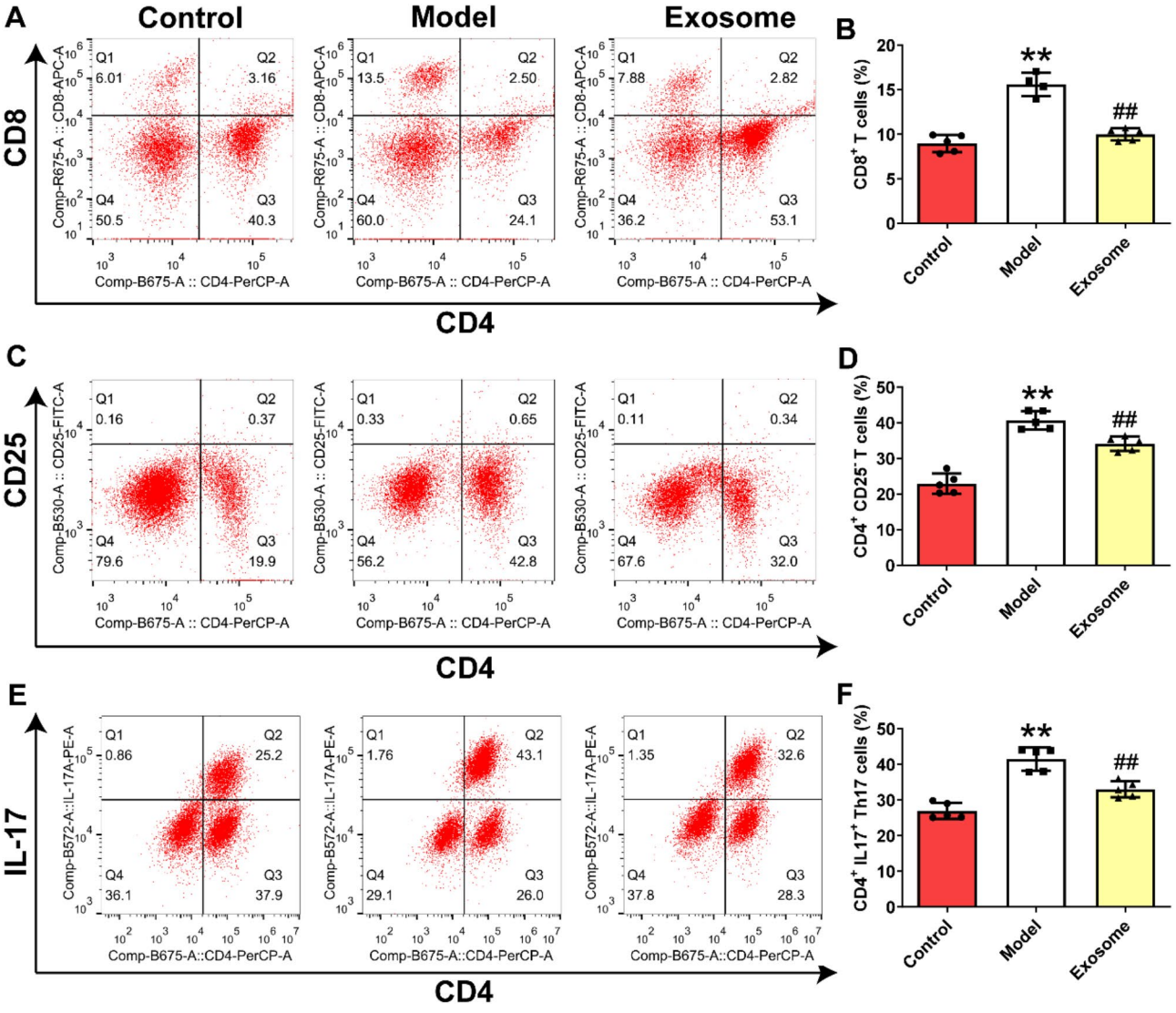

Fig. 3 Flow cytometry analysis for lymphocyte immunophenotyping from Sprague Dawley rats. (**A**) Flow quadrant diagram of CD4 and CD8. (**B**) Proportion of $CD8^+$ T cells (quadrant 1 + 2 in A). (**C**) Flow quadrant diagrams of CD4 and CD25. (**D**) Proportion of $CD4^+$ T-cells (quadrant 2 + 3 in C). (**E**) Flow quadrant diagrams of CD4 and IL-17. (**F**) Proportion of $CD4^+$ IL-17^+ T cells (quadrant 2 in **F**). $n = 6$. The "*n*" means number of animals. Mean ± standard deviation, one-way analysis of variance was used for statistical analysis. $^{**}p < 0.01$ vs. control group; $^{\#\#}p < 0.01$ vs. model group

of Th17-related cytokines in endothelial cell activation led to tissue remodeling in the bronchi [10]. This COPD model was characterized by significant inflammatory cell infiltration and tissue remodeling, evident through HE staining. Notably, smooth muscle cell proliferation and bronchial atrophy were observed, and airway patency measures such as PEF showed a significant decrease, while the proxy for airway obstruction, RI, showed a substantial increase. Moreover, research has shown that smoking can stimulate a range of immune responses, which can trigger tissue repair and reconstruction [2, 30]. Therefore, we proposed that exosomes may be able to mitigate pulmonary function damage caused by COPD by inhibiting inflammation.

The correlation between exosomes produced by immune cells and the intensity of immune responses has been widely accepted [16]. Th17s and their production of pro-inflammatory cytokines are critical factors in inflammation [10]. Th17s markedly increased in patients with COPD compared to health control [31], suggesting Th17 may play a key pro-inflammatory role in COPD. Furthermore, $CD8^+$ T cells have been implicated in inflammation and lung destruction in a mouse model of cigarette smoke-induced emphysema [32]. In our experiments, we observed a Th17s and $CD8^+$ cells increased in COPD rats while Treg-exo inhibited them. These results were consistent with the conclusion of the previous research, which supports our hypothesis that Treg-exo can mitigate lung tissue damage of COPD, which maybe

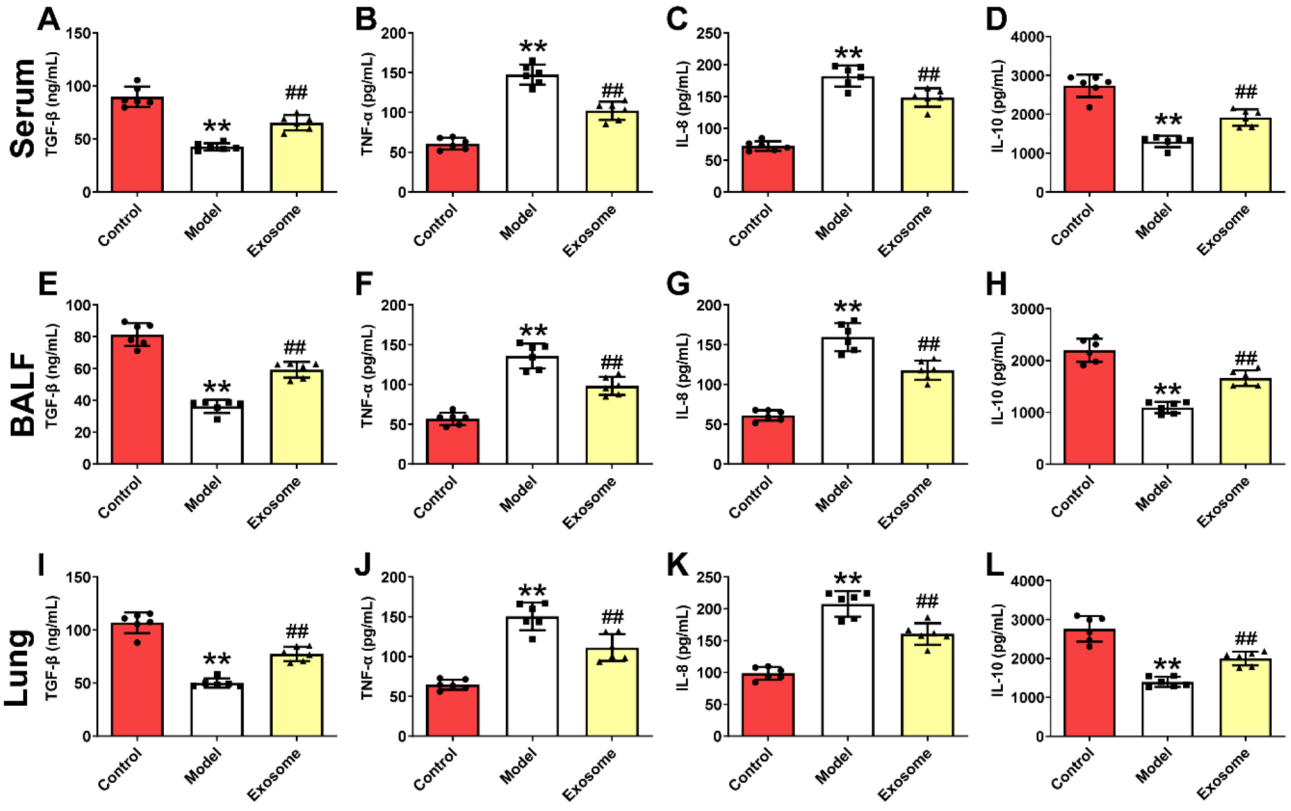

Fig. 4 Content of cytokines in serum, BALF, and lung tissue from Sprague Dawley rats. (**A**-**D**) Content of (**A**) TGF-β, (**B**) TNF-α, (**C**) IL-8, and (**D**) IL-10 in serum; (**E**-**H**) Content of (**E**) TGF-β, (**F**) TNF-α, (**G**) IL-8, and (**H**) IL-10 in BALF; (**I**-**L**) Content of (**I**) TGF-β, (**J**) TNF-α, (**K**) IL-8, and (**I**) IL-10 in lung tissue. $n = 6$. The "*n*" means number of animals. Mean ± standard deviation, one-way analysis of variance was used for statistical analysis. TGF-β, transforming growth factor-β; TNF-α, tumor necrosis factor-α; IL, interleukin; BALF, broncho alveolar lavage fluid. $^{**}p < 0.01$ vs. control group; $^{\#\#}p < 0.01$ vs. model group

achieve by inhibiting immune inflammation and T cell differentiation.

Furthermore, our subsequent analysis of inflammatory cytokines revealed that Treg-exo promotes IL-10 and inhibits TNF-α and IL-8. Consistent with us, TNF-α and IL-8 were significantly increased in the COPD rat model, while IL-10 expression was the opposite [33, 34]. Research has reported that IL-8 and TNF-α are associated with the activation of Th17s; Additionally, the cytokine IL-17 secreted by Th17s can also stimulate fibroblasts to secrete IL-8 [35]. Additionally, IL-10 is a cytokine related to Tregs and typically exerts an anti-inflammatory effect [36]. Its upregulation may be attributed to the infusion of Treg-exo, thereby playing an anti-inflammatory role. The levels of these cytokines support the importance of immune cells in COPD, especially Th17 and Tregs.

A clinical analysis shows that total plasma TGF-β1 (contained both the active and latent forms of TGF-β1) higher in patients with COPD, however, its active form levels did not show differ significantly [31]. TGF-β1 knockout induced severe inflammation in multiple organs, including lung [37]. Paradoxically, in rats exposed to COPD for 24 weeks, serum and BALF TGF-β1 levels were increased [33]. Contrary to these findings, we observed a downregulation of the total TGF-β level in COPD rats. Given that our modeling period was only 5 weeks, it is highly likely that the insufficient modeling time contributed to this discrepancy. This suggests that the immune response involving TGF-β may be related to the reaction time. In addition, past research has revealed that there are conduction disorders in the TGF-β/Smad signaling pathway in COPD [31]. Notably, TGF-β exists in different forms and exhibits diverse biological functions in various environments [37]. Therefore, there may be negative feedback regulations involved in the TGF-β-related signaling pathways. In the future, more experiments may be needed to clarify the roles of TGF-β with different activities during different stages of COPD development.

In addition, although the specific mechanism of interaction between Th17s has not been fully elucidated, published research indicates that Th17s secrete a range of cytokines, including IL-17, which are capable of acting on other cell types. Consequently, these cytokines can stimulate a range of specific immune responses [38]. Studies have demonstrated that CXCL8, also referred to as IL-8, can stimulate the expression of IL-17 and be involved

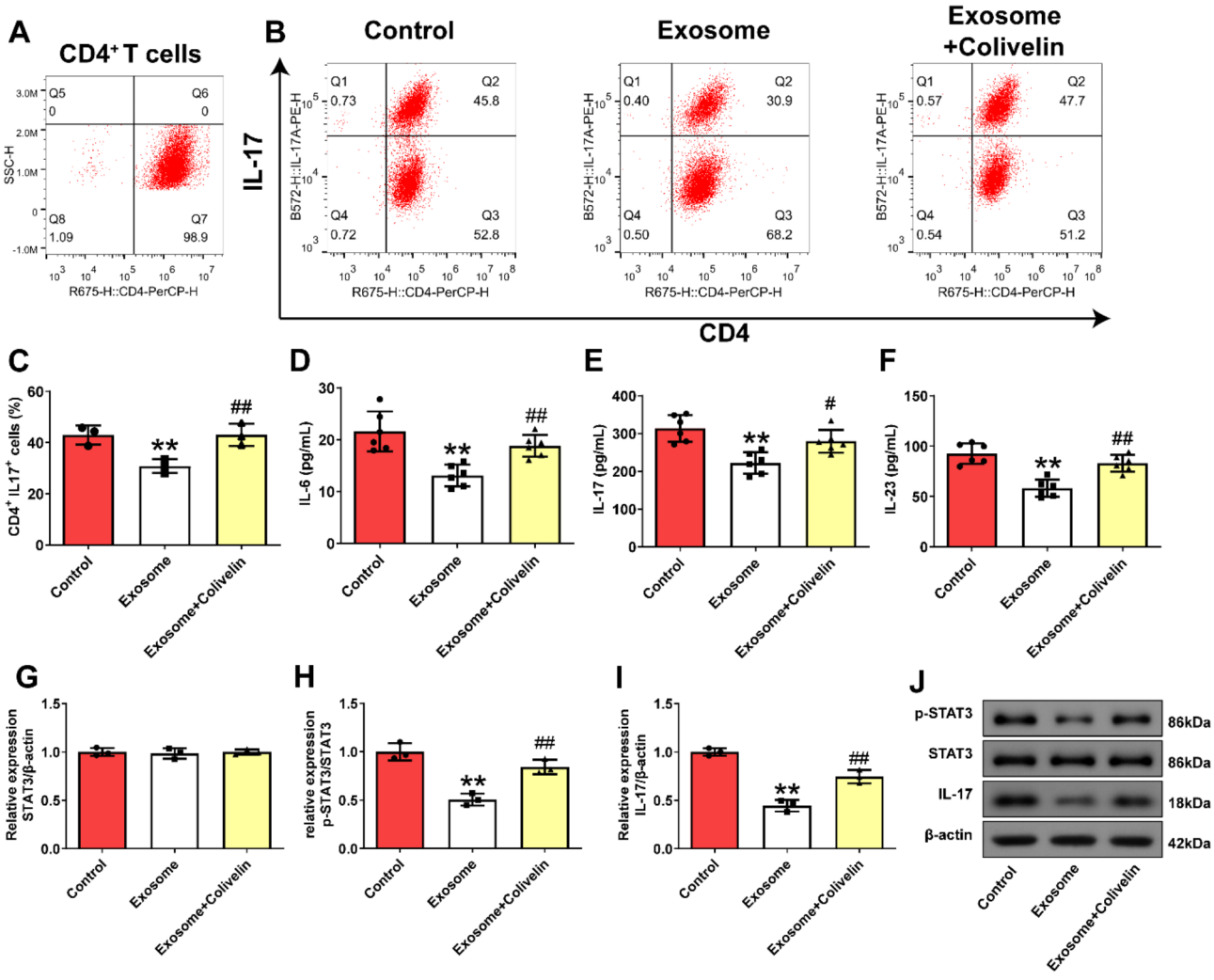

Fig. 5 The effect of normal Treg-exo on CD4 + T-cells from spleen of COPD rats. (**A**) Flow cytometry assay was used for $CD4^+$ T-cell identification, $n = 3$. (**B**) Flow cytometry was used for Th17 ($CD4^+$ $IL\text{-}17^+$ cells) identification and $CD4^+$ $IL\text{-}17^+$ cells proportion analysis, $n = 3$. (**D**-**F**) The contents of (**D**) IL-6, (**E**) IL-17, and (**F**) IL-23 were detected using ELISA. $n = 6$. (**G**-**I**) The relative expressions of (**G**) STAT3, (**H**) p-STAT3, and (**I**) IL-17 were measured using Western blot. $n = 3$. (**J**) Representative image of protein bands. $n = 3$. The "*n*" means number of experimental replicates. Mean ± standard deviation, one-way analysis of variance was used for statistical analysis. $^{**}p < 0.01$ vs. control group; $^{\#}p < 0.05$, $^{\#\#}p < 0.01$ vs. model group

in the regulation of adhesion molecules in stromal cells such as fibroblasts and endothelial cells [39, 40]. IL-6 and TNF-α are inflammatory cytokines that play a key role in regulating immunity and are primarily secreted by Th17s, which are known to prime the innate immune system and drive the initiation of autoimmunity [38].Relevant evidence revealed that treatment with exosomes derived from Tregs efficiently diminished the Th17 subset's growth, resulting in pronounced reductions in IL-8 and TNF-α, two pro-inflammatory cytokines. Consequently, these exosomes were effective in suppressing inflammation and preventing further damage to lung tissue.

Furthermore, research has shown that STAT3 is involved in an interaction with IL-17. Generally speaking, STAT3 is activated by cytokines, including IL-6, IL-17, IL-23, TGF-β, and IL-1β, released by mature APC cells. However, activated STAT3 drives the differentiation of naive $CD4^+$ T-cells towards Th17, thus regulating IL-17 production [41]. For example, Li revealed that extracellular vesicles derived from mesenchymal stem cells can inhibit Th17 differentiation, possibly by inhibiting the IL-6/STAT3/IL-17 signaling pathway [42]. Simultaneously, we also found significant decreases in IL-6, IL-17, and IL-23 levels, along with reduced STAT3 phosphorylation following Treg-exo treatment. Furthermore, upon exposure to STAT3 activator Colivelin, the suppressive effects of Treg-exo were partially reversed. Based on these observations, we hypothesized that Treg-exo may also inhibit Th17 differentiation by interfering with the STAT3/IL-17 signaling pathway.

This study serves as a preliminary exploration of the beneficial effects of Treg-exo and its underlying

mechanisms, and it has confirmed the beneficial effects of Treg-exo. However, the specific mechanisms still require further in-depth research for conclusive evidence. This study has shown that the STAT3-related signaling pathway might be involved in what Tregs-exo does. But this is just the beginning. It gives us a good direction to figure out how things work. However, pharmacological intervention is not enough to clarify the target effects of Tregs-exo on the STAT3 signaling pathway. More in-depth exploration is needed. In the future, we will focus on the effects of Treg-exo in different COPD models, as well as the STAT3 signaling pathway.

Conclusions

In conclusion, we determined that Treg-exo treatment protected lung tissue integrity and pulmonary function from inflammatory, which is the main cause of COPD. Moreover, the alteration of cytokines content and T lymphocyte subsets suggested that exosomes may suppress inflammatory via affecting $CD4^+$ T-cells differentiation by inhibiting STAT3.

Abbreviations

Treg-exo	Exosomes derived from Tregs
COPD	Chronic obstructive pulmonary disease
EMT	Epithelial-mesenchymal transition
TEM	Transmission electron microscope
PEF	Peak expiratory flow
RI	Airway resistance
FRC	Functional residual capacity
Cdyn	Dynamic lung compliance
BALF	Bronchoalveolar lavage fluid
TGF-β	Transforming growth factor-β
TNF-α	Tumor necrosis factor-α
IL	Interleukin

Supplementary Information

The online version contains supplementary material available at https://doi.org/10.1186/s12890-025-03632-x.

Supplementary Material 1

Acknowledgements

Not applicable.

Author contributions

Xuefang Tao: Conceptualization, Formal analysis, Funding acquisition, Investigation, Project administration, Writing-original draft. Hai Tian: Data curation, Formal analysis, Investigation, Methodology. Guowen Wang: Data curation, Formal analysis, Investigation, Visualization. Yongzhen Sun: Investigation, Methodology, Validation, Visualization. Liangyan Zhao: Conceptualization, Project administration, Supervision, Writing-review & editing.

Funding

This study was supported by the Zhejiang Province Basic Commonweal Research Project [grant number LGF22H010004].

Data availability

The datasets used and/or analysed during the current study are available from the corresponding author on reasonable request.

Declarations

Ethics approval and consent to participate

The Animal Experimentation Ethics Committee of Zhejiang Eyong Pharmaceutical Research and Development Center approved the ethical conduct of the animal experiments (approval number: ZJEY-20220818-01).

Consent for publication

Not applicable.

Competing interests

The authors declare no competing interests.

Author details

[1]Department of Respiratory Medicine, The Affiliated Hospital of ShaoXing University, No. 999, Zhongxing South Road, Yuecheng District, Shaoxing 312000, Zhejiang, China
[2]Department of Basic Medicine, Medical College, Shaoxing University, Shaoxing 312000, Zhejiang, China

Received: 10 January 2025 / Accepted: 27 March 2025
Published online: 14 April 2025

References

1. Wang Y, Zhang N, Liu F, Zhou J, Teng G, Huang H. A new perspective for improving COPD: ginsenoside Rg3 links SIRT1 to inhibit mitochondrial autophagy. Discov Med. 2024;36:2386–98. https://doi.org/10.24976/Discov.Med.202436191.220.
2. Hikichi M, Mizumura K, Maruoka S, Gon Y. Pathogenesis of chronic obstructive pulmonary disease (COPD) induced by cigarette smoke. J Thorac Disease. 2019;11:S2129–40. https://doi.org/10.21037/jtd.2019.10.43.
3. Gao H, Song Y, Liu K, Lu X, Shen J, Wei S, et al. The impact of different smoking behavior on pulmonary function and pulmonary hypertension among Chinese male patients with chronic obstructive pulmonary disease. Int J Chronic Obstr Pulm Dis. 2024;19:1315–31. https://doi.org/10.2147/copd.S455323.
4. Almagro P, Boixeda R, Diez-Manglano J, Gómez-Antúnez M, López-García F, Recio J. Insights into chronic obstructive pulmonary disease as critical risk factor for cardiovascular disease. Int J Chronic Obstr Pulm Dis. 2020;15:755–64. https://doi.org/10.2147/copd.S238214.
5. Lin L, Li J, Song Q, Cheng W, Chen P. The role of HMGB1/RAGE/TLR4 signaling pathways in cigarette smoke-induced inflammation in chronic obstructive pulmonary disease. Immun Inflamm Dis. 2022;10:e711. https://doi.org/10.1002/iid3.711.
6. Machida H, Inoue S, Igarashi A, Saitoh S, Yamauchi K, Nishiwaki M, et al. Role of CC chemokine ligand 17 in mouse models of chronic obstructive pulmonary disease. Am J Respir Cell Mol Biol. 2022;66:428–38. https://doi.org/10.1165/rcmb.2021-0069OC.
7. Du Y, Ding Y, Shi T, He W, Mei Z, Feng X, et al. Suppression of circXPO1 attenuates cigarette smoke-induced inflammation and cellular senescence of alveolar epithelial cells in chronic obstructive pulmonary disease. Int Immunopharmacol. 2022;111:109086. https://doi.org/10.1016/j.intimp.2022.109086.
8. Fang L, Sun Q, Roth M. Immunologic and Non-Immunologic mechanisms leading to airway remodeling in asthma. Int J Mol Sci. 2020;21:757. https://doi.org/10.3390/ijms21030757.
9. Jiang Z, Zhang Y, Zhu Y, Li C, Zhou L, Li X, et al. Cathelicidin induces epithelial-mesenchymal transition to promote airway remodeling in smoking-related chronic obstructive pulmonary disease. Annals Translational Med. 2021;9:223. https://doi.org/10.21037/atm-20-2196.
10. Di Stefano A, Caramori G, Gnemmi I, Contoli M, Vicari C, Capelli A, et al. T helper type 17-related cytokine expression is increased in the bronchial mucosa of stable chronic obstructive pulmonary disease patients. Clin Exp Immunol. 2009;157:316–24. https://doi.org/10.1111/j.1365-2249.2009.03965.x.
11. Bruzzaniti SB, Santopaolo M, Calì M, Stanziola G, D'Amato AA, Esposito M, Barra A, Garziano E, Micillo F, Zuchegna T, Romano C, De Simone A, Zuccarelli S, Mottola B, De Rosa M, Porcellini V, Perna A, Matarese F, Galgani G. Mario;. An immunometabolic pathomechanism for chronic obstructive pulmonary disease. Proc Natl Acad Sci U S A 2019; 116. https://doi.org/10.1073/pnas.1906303116

12. Keru Q, Baixue, Xu, Min, Pang H, Baofeng W. Yu,. The functions of CD4 T-helper lymphocytes in chronic obstructive pulmonary disease. Acta Biochim Biophys Sin (Shanghai) 2022; 54. https://doi.org/10.3724/abbs.2021009
13. Xiao D, Li S, Gui B, Han J, Duan Z, Jia L, et al. Effect of uremic serum on Th17/Treg cell balance and Endoplasmic reticulum stress in rats. Biomed Pharmacother. 2020;131:110705. https://doi.org/10.1016/j.biopha.2020.110705.
14. Qin K, Xu B, Pang M, Wang H, Yu B. The functions of CD4 T-helper lymphocytes in chronic obstructive pulmonary disease. Acta Biochim Biophys Sin. 2022;54:173–8. https://doi.org/10.3724/abbs.2021009.
15. Williams M, Todd I, Fairclough L. The role of CD8 + T lymphocytes in chronic obstructive pulmonary disease: a systematic review. Inflamm Research: Official J Eur Histamine Res Soc. 2021;70:11–8. https://doi.org/10.1007/s00011-020-01408-z.
16. Anel A, Gallego-Lleyda A, De Miguel D, Naval J, Martínez-Lostao L. Role of exosomes in the regulation of T-Cell mediated immune responses and in autoimmune disease. Cells. 2019;8:154. https://doi.org/10.3390/cells8020154.
17. Kim J, Kim T, Lee M, Mun J, Ihm C, Kim S. Exosome cargo reflects TGF-β1-mediated epithelial-to-mesenchymal transition (EMT) status in A549 human lung adenocarcinoma cells. Biochem Biophys Res Commun. 2016;478:643–8. https://doi.org/10.1016/j.bbrc.2016.07.124.
18. Guo H, Fei L, Yu H, Li Y, Feng Y, Wu S, et al. Exosome-encapsulated LncRNA HOTAIRM1 contributes to PM-aggravated COPD airway remodeling by enhancing myofibroblast differentiation. Sci China Life Sci. 2024;67:970–85. https://doi.org/10.1007/s11427-022-2392-8.
19. Pang X, Wang Z, Liu L, Feng Y, Wang J, Xie H, et al. Immature dendritic cells derived exosomes promotes immune tolerance by regulating T cell differentiation in renal transplantation. Aging. 2019;11:8911–24. https://doi.org/10.18632/aging.102346.
20. Xu Z, Zhang H, Li W, Ran Y, Liu T, Xiong M, et al. FAM64A positively regulates STAT3 activity to promote Th17 differentiation and colitis-associated carcinogenesis. Proc Natl Acad Sci USA. 2019;116:10447–52. https://doi.org/10.1073/pnas.1814336116.
21. He Y, Li M, Wujisiguleng, Lv B, Huan Y, Liu B, et al. Zhenbao pill reduces Treg cell proportion in acute spinal cord injury rats by regulating TUG1/miR-214/HSP27 axis. Biosci Rep. 2018;38:BSR20180895. https://doi.org/10.1042/bsr20180895.
22. Kaewsakulthong W, Suriyun T, Chumchuen SA-O, Anurathapan UA-O, Hongeng SA-O, Fucharoen S, et al. In vitro study of ineffective erythropoiesis in thalassemia: diverse intrinsic pathophysiological features of erythroid cells derived from various thalassemia syndromes. J Clin Med. 2022;11:5356. https://doi.org/10.3390/jcm11185356.
23. Yuan D, Chen H, Wang S, Liu F, Cheng Y, Fang JA-O. Identification of LEA, a podocalyxin-like glycoprotein, as a predictor for the progression of colorectal cancer. Cancer Med. 2018;7:5155–66. https://doi.org/10.1002/cam4.1765.
24. Jia Y, He T, Wu D, Tong J, Zhu J, Li Z, et al. The treatment of Qibai Pingfei capsule on chronic obstructive pulmonary disease May be mediated by Th17/Treg balance and gut-lung axis microbiota. J Transl Med. 2022;20:281. https://doi.org/10.1186/s12967-022-03481-w.
25. Yu X, Huang C, Song B, Xiao Y, Fang M, Feng J, et al. CD4 + CD25 + regulatory T cells-derived exosomes prolonged kidney allograft survival in a rat model. Cell Immunol. 2013;285:62–8. https://doi.org/10.1016/j.cellimm.2013.06.010.
26. Kong J, Wang F, Zhang J, Cui Y, Pan L, Zhang W, et al. Exosomes of endothelial progenitor cells inhibit Neointima formation after carotid artery injury. J Surg Res. 2018;232:398–407. https://doi.org/10.1016/j.jss.2018.06.066.
27. Serwas NK, Hoeger B, Ardy RC, Stulz SV, Sui Z, Memaran N, et al. Human DEF6 deficiency underlies an immunodeficiency syndrome with systemic autoimmunity and aberrant CTLA-4 homeostasis. Nat Commun. 2019;10:3106. https://doi.org/10.1038/s41467-019-10812-x.
28. Zhao X, Li N, Yang N, Mi B, Dang W, Sun D, et al. Thymosin B4 alleviates autoimmune dacryoadenitis via suppressing Th17 cell response. Investig Ophthalmol Vis Sci. 2023;64:3. https://doi.org/10.1167/iovs.64.11.3.
29. Lopez-Campos J, Calero-Acuña C, Lopez-Ramirez C, Abad-Arranz M, Márquez-Martín E, Ortega-Ruiz F, et al. Implications of the inflammatory response for the identification of biomarkers of chronic obstructive pulmonary disease. Biomark Med. 2016;10:109–22. https://doi.org/10.2217/bmm.15.87.
30. Nowrin K, Sohal S, Peterson G, Patel R, Walters E. Epithelial-mesenchymal transition as a fundamental underlying pathogenic process in COPD airways: fibrosis, remodeling and cancer. Expert Rev Respir Med. 2014;8:547–59. https://doi.org/10.1586/17476348.2014.948853.
31. Zhang JC, Chen G, Chen L, Meng ZJ, Xiong XZ, Liu HJ, et al. TGF-β/BAMBI pathway dysfunction contributes to peripheral Th17/Treg imbalance in chronic obstructive pulmonary disease. Sci Rep. 2016;6:31911. https://doi.org/10.1038/srep31911.
32. Maeno T, Houghton A, Quintero P, Grumelli S, Owen C, Shapiro S. CD8 + T cells are required for inflammation and destruction in cigarette smoke-induced emphysema in mice. J Immunol (Baltimore Md: 1950). 2007;178:8090–6. https://doi.org/10.4049/jimmunol.178.12.8090.
33. Mohammadtursun N, Li Q, Abuduwaki M, Jiang S, Zhang H, Sun J, et al. Loki Zupa alleviates inflammatory and fibrotic responses in cigarette smoke induced rat model of chronic obstructive pulmonary disease. Chin Med. 2020;15:92. https://doi.org/10.1186/s13020-020-00373-3.
34. Wang D, Du Q, Li H, Wang S. The isosteroid alkaloid imperialine from bulbs of fritillaria cirrhosa mitigates pulmonary functional and structural impairment and suppresses inflammatory response in a COPD-Like rat model. Mediators Inflamm. 2016;2016:4192483. https://doi.org/10.1155/2016/4192483.
35. Burns LA, Maroof A, Marshall D, Steel KJA, Lalnunhlimi S, Cole S, et al. Presence, function, and regulation of IL-17F-expressing human CD4(+) T cells. Eur J Immunol. 2020;50:568–80. https://doi.org/10.1002/eji.201948138.
36. Zhao P, Li J, Tian Y, Mao J, Liu X, Feng S, et al. Restoring Th17/Treg balance via modulation of STAT3 and STAT5 activation contributes to the amelioration of chronic obstructive pulmonary disease by bufei Yishen formula. J Ethnopharmacol. 2018;217:152–62. https://doi.org/10.1016/j.jep.2018.02.023.
37. Saito A, Horie M, Nagase T. TGF-β signaling in lung health and disease. Int J Mol Sci. 2018;19. https://doi.org/10.3390/ijms19082460.
38. Traves S, Donnelly L. Th17 cells in airway diseases. Curr Mol Med. 2008;8:416–26. https://doi.org/10.2174/156652408785160998.
39. Chizzolini C, Dufour A, Brembilla N. Is there a role for IL-17 in the pathogenesis of systemic sclerosis? Immunol Lett. 2018;195:61–7. https://doi.org/10.1016/j.imlet.2017.09.007.
40. Matsuzaki G, Umemura M. Interleukin-17 as an effector molecule of innate and acquired immunity against infections. Microbiol Immunol. 2007;51:1139–47. https://doi.org/10.1111/j.1348-0421.2007.tb04008.x.
41. Qin Z, Wang R, Hou P, Zhang Y, Yuan Q, Wang Y, et al. TCR signaling induces STAT3 phosphorylation to promote TH17 cell differentiation. J Exp Med. 2024;221:e20230683. https://doi.org/10.1084/jem.20230683.
42. Li C, Wu F, Mao J, Wang Y, Zhu J, Hong K, et al. Mesenchymal stem cells-derived extracellular vesicles ameliorate lupus nephritis by regulating T and B cell responses. Stem Cell Res Ther. 2024;15:216. https://doi.org/10.1186/s13287-024-03834-w.

Publisher's note